Increased expression of integrin-linked kinase during decidualization regulates the morphological transformation of endometrial stromal cells

Chih-Feng Yen, M.D., Ph.D.,[a,b] Sung Hoon Kim, M.D., Ph.D.,[c] Shuen-Kuei Liao, Ph.D.,[b,d] Cem Atabekoglu, M.D.,[e] Serpil Uckac, M.Sc.,[f] Aydin Arici, M.D.,[f] Sefa Arlier, M.D.,[g] Chyi-Long Lee, M.D., Ph.D.,[h] Hsin-Shih Wang, M.D., Ph.D.,[a,b] and Umit A. Kayisli, Ph.D.[g]

[a] Department of Obstetrics and Gynecology, Chang Gung Memorial Hospital at Linkou and Chang Gung University College of Medicine, Kwei-Shan, Tao-Yuan, Taiwan; [b] Graduate Institute of Clinical Medical Sciences, Chang Gung University College of Medicine, Taoyuan, Taiwan; [c] Department of Obstetrics and Gynecology, University of Ulsan College of Medicine, Asan Medical Center, Seoul, South Korea; [d] Ph.D. Program of Cancer Biology and Drug Discovery, and Center of Excellence for Cancer Research, Taipei Medical University, Taipei, Taiwan; [e] Department of Obstetrics and Gynecology, Ankara University School of Medicine, Ankara, Turkey; [f] Department of Obstetrics, Gynecology and Reproductive Sciences, Yale University School of Medicine, New Haven, Connecticut; [g] Department of Obstetrics and Gynecology, Morsani College of Medicine, University of South Florida, Tampa, Florida; and [h] Department of Obstetrics and Gynecology, Keelung Chang Gung Memorial Hospital and Chang Gung University College of Medicine, Keelung, Taiwan

Objective: To study the impact of integrin-linked kinase (ILK) in endometrial stromal cells (ESCs) during decidualization.
Design: Laboratory study with the use of human endometrium.
Setting: University hospital.
Patient(s): Fertile reproductive-age women who had not received hormonal treatment for 3 months before tissue collection.
Intervention(s): Endometrium tissue collection, in vitro decidualization of isolated ESCs, and small interfering (si) RNA transfection.
Main Outcome Measure(s): Immunohistochemistry, ELISA, Western blot analysis, methylthiazolyl tetrazolium assay, and immunofluorescence staining.
Result(s): In vivo expression of ILK is significantly increased in distended-fusiform stromal cells of late secretory endometrium and in cobblestone-shaped decidual cells of early pregnancy. During in vitro decidualization for up to 8 days, confluent cultures of isolated ESCs consistently displayed increased ILK expression and morphologic transformation from fibroblast-like to polygonal cells. Subsequent ILK knockdown by siRNA transfection reversed this transformation, accompanied by decreased phosphorylation of glycogen synthase kinase (GSK) 3β and decreased viable cell numbers. Immunofluorescence staining of the decidualized ESCs demonstrated linkage of increased levels of ILK at the tips of the fan-shaped organization of actin stress fibers located in the submembranous area, which expanded the decidual cells into a typical polygonal appearance. Knock-down of ILK abrogated the polymerization and organization of actin fibers, which reverted the cells to their undecidualized morphology.
Conclusion(s): During human endometrial decidualization, ILK is essential for morphologic transformation of ESCs through organization of the actin cytoskeleton; it may also function through subsequent GSK3β signaling, which requires further studies. (Fertil Steril® 2017;107:803–12. ©2016 by American Society for Reproductive Medicine.)
Key Words: Integrin-linked kinase, decidualization, endometrium, actin

Discuss: You can discuss this article with its authors and with other ASRM members at https://www.fertstertdialog.com/users/16110-fertility-and-sterility/posts/13551-22579

Received June 10, 2016; revised November 19, 2016; accepted November 28, 2016; published online January 6, 2017.
C.-F.Y. has nothing to disclose. S.H.K. has nothing to disclose. S.-K.L. has nothing to disclose. C.A. has nothing to disclose. S.U. has nothing to disclose. A.A. has nothing to disclose. S.A. has nothing to disclose. C.-L.L. has nothing to disclose. H.-S.W. has nothing to disclose. U.A.K. has nothing to disclose.
Supported in part by research grants from the Ministry of Science and Technology of Taiwan (NMRPG496031, 99-2314-B-182A-048-MY2) and Chang Gung Medical Foundation (CMRPG3C0673) (to C.-F.Y.).
C.-F.Y. and S.H.K. should be considered similar in author order.
This study is part of the Ph.D. dissertation of C.-F.Y.
Previously presented at the 54th Annual Scientific Meeting of the Society for Reproductive Investigation, Reno, Nevada, March 14–17, 2007.
Reprint requests: Umit A. Kayisli, Ph.D., Department of Ob/Gyn, College of Medicine, University of South Florida, Tampa, FL (E-mail: uakayisli@health.usf.edu).

Fertility and Sterility® Vol. 107, No. 3, March 2017 0015-0282/$36.00

http://dx.doi.org/10.1016/j.fertnstert.2016.11.025

In preparation for embryo implantation, the endometrium undergoes decidualization, a process that involves tissue remodeling, which includes molecular differentiation, morphologic transformation, and extracellular matrix (ECM) reorganization and integrin switching (1).

Integrins act as prototypic heterodimeric transmembrane receptors for ECM proteins to induce formation of focal adhesions (2). Integrin-linked kinase (ILK) is a key scaffold protein localized within focal adhesions where it acts as a central component of a heterotrimer (the ILK-PINCH-parvin complex) (3). Since its discovery, ILK has demonstrated an essential role in connecting the cytoplasmic tail of integrin β_1 and β_3 to the actin cytoskeleton and regulating actin polymerization (4).

ILK occupies a pivotal position in cell-matrix adhesion and can activate the transmembrane signals bidirectionally (5, 6). By down-regulating E-cadherin expression (7), ILK acts as a mediator of epithelial-to-mesenchymal transition, which plays important roles in embryo development and cancer progression (8–11). Corroboratively, aberrantly overexpressed or -activated ILK has been demonstrated in many types of human malignancies (3), and ILK-knockout mice die shortly after implantation owing to the defective epiblast polarization and abnormal F-actin accumulation (12). ILK can also behave as a multifunctional serine/threonine kinase to transmit its signal in a phosphatidylinositol 3-kinase–dependent manner (13, 14) through phosphorylating protein kinase B (Akt1), and/or glycogen synthase kinase-3β (GSK3β) pathways, which enable it to regulate such processes as cell proliferation, survival, migration, and invasion (15).

The role of ILK in reproductive sciences has been underexplored. In patients with preeclampsia, the expression of ILK and the number of endothelial progenitor cells are diminished (16). A recent study observed increased ILK expression in endometrial stromal cells (ESCs) of women with endometriosis and suggested a correlation with the increased migration and invasion functions of these cells in such patients (17). A separate study observed that ILK is highly expressed on the plasma membranes of extravillous trophoblast cells and that ILK may enhance the migration of chorionic villi (15). However, no study has focused on the potential roles of ILK in endometrium, although three integrins, $\alpha1\beta1$, $\alpha4\beta1$, and $\alpha v\beta3$, are coexpressed during the window of implantation (18–20), which suggests the possible involvement of ILK in decidualization and implantation. In view of the well documented occurrence of morphologic changes of ESCs during decidualization, we hypothesized that ILK expression could contribute to specific decidualization-related cellular functions and performed experiments to test this hypothesis.

MATERIALS AND METHODS

The study protocols were reviewed and approved by the Human Investigation Review Board of Yale University and Linkou Chang Gung Memorial Hospital, Taiwan. Written informed consent was obtained from every patients before surgery and tissue collection.

Patients and Tissue Specimens

Endometrial tissues were obtained from surgical specimens of fertile women with regular menstrual cycles who underwent laparoscopy or hysterectomy (21, 22) for benign gynecologic conditions, without endometriosis, adenomyosis, or hyperplastic endometrial disease, and who did not receive hormonal medication in the preceding 3 months. For immunohistochemical staining ($n = 5$ for each menstrual phase; total $n = 30$; mean age 40.4 years, range 23–48), the date of the menstrual cycle was classified as early proliferative (days 1–5), midproliferative (days 6–10), late proliferative (days 11–14), early secretory (days 15–18), midsecretory (days 19–23), and late secretory (days 24–28) phases, according to menstrual history and confirmed by means of endometrial histology with the use of the criteria of Noyes et al. (23). Decidual tissues ($n = 5$ for immunohistochemistry; $n = 3$ for decidual cell culture) were collected from voluntary terminations of normal pregnancies during the first trimester.

Endometrial tissue for ESC isolation and long-term culture ($n = 23$) was also obtained from surgical specimens of fertile women with the use of the same criteria as mentioned above, and placed in Hank balanced salt solution (HBSS; Sigma-Aldrich). Despite isolation from different menstrual cycle stages, study showed that ESCs by passage 2 did not differ in the expression of cycle-specific genes and were naïve (or without memory) in their response in the experimental treatment protocols (24).

Immunohistochemistry

Formalin-fixed paraffin-embedded specimens were cut into 5-μm sections. After deparaffinization, antigen retrieval was performed by boiling in citrate buffer (10 mmol/L, pH 6.0) for 15 minutes, and endogenous peroxidase was blocked by means of immersion in 3% hydrogen peroxide (in 50% methanol:50% distilled water solution) for 12 minutes. Slides were then incubated in a humidified chamber with 5% normal horse serum (Vector Laboratories) in Tris-buffered saline solution (TBS; 0.05 mol Tris [pH 7.4], 0.85% saline) for 30 minutes at room temperature. After drainage of excess serum, sections were incubated with a 1:6,000 dilution (0.33 μg/mL) of mouse monoclonal anti–human ILK antibody (Sigma) overnight at 4°C in a humidified chamber. Nonimmune (normal) mouse IgG1 was used at the same concentration of the primary antibody for isotype control samples. With the use of the horse anti–mouse biotinylated secondary antibody (Vector Laboratories), the antigen-antibody complex was detected by means of the avidin-biotin-peroxidase complex (Vectastain ABC kit; Vector Laboratories) and 3,3′-diaminobenzidine tetrahydrochloride (Sigma-Aldrich) with light hematoxylin counterstaining. Images were collected at room temperature with the use of an Axioplan 2 Imaging (Carl Zeiss) microscope with an Axiocam (Zeiss) camera, and Axiovison (release 4.6; Zeiss) software.

Immunoreactivity was evaluated by means of H-score in an area of containing ~100 cells (×400), with the use of the formula: H-score = ΣP_i (intensity score), where the intensity score is graded as 0 for none, 1 for weak but detectable, 2 for moderate or distinct staining, or 3 for strong staining, and P_i is the corresponding percentage (range 0–100) of the positively stained cells in each category and therefore yielding a value ranging from 0 to 300 (25). The final average scores

were obtained from five fields per slide and evaluated by two investigators blinded to the tissue source.

Isolation and Culture of Human ESCs

Fresh endometrial tissue was minced and digested in HBSS (Sigma-Aldrich) containing collagenase B (15 U mg/mL; Roche), deoxyribonuclease I (150 U/mL; Roche), penicillin (200 U/mL), and streptomycin (200 mg/mL) for 60 minutes at 37°C with gentle agitation. Human ESCs were separated by means of a wire sieve (40-μm-diameter pore; BD) and cultured in Dulbecco Modified Eagle Medium (DMEM)/Ham F-12 (1:1 vol/vol; Sigma) containing fetal bovine serum (FBS, 10% vol/vol; Gibco BRL) until confluent. After the first passage, immunohistochemical assessment of ESCs were previously found to contain 0%–3% epithelial cells, no detectable endothelial cells, and 0.2% macrophages (26, 27).

Experimental Incubation

ESCs (passage 3–5) grown to 70% confluence were then starved for 24 hours in serum-free basal medium, a phenol red–free DMEM/Ham F-12 nutrient mixture (1:1 vol/vol; Sigma) medium with 100 U/mL penicillin, 100 g/mL streptomycin, 0.25 g/mL fungizone. To test the nongenomic actions of steroid hormones (28), cultures were incubated in parallel in basal medium supplemented with 10% charcoal-stripped fetal calf serum (Biological Industries, Beit Haemek, Israel) containing either 0.1% ethanol, as vehicle control, or E_2 (10^{-8} mol/L; Sigma), or P (10^{-7} mol/L; Sigma), or E_2 + P for 15 minutes, 45 minutes, 24 hours, and 48 hours. For in vitro decidualization, cultures were treated with E_2 + P in basal medium with serum (BMS) for 2, 4, 6, 8, 10, and 12 days. Prolactin levels in the supernate was determined as a biomarker of decidualization with the use of a commercially available ELISA kit (Advia Centaur XP systems; Siemens; Intra-assay range 0.3–200 ng/mL) per the manufacturer's instructions.

Small Interfering RNA Transfection

All small interfering (si) RNA kits were purchased from Cell Signaling. ESCs and decidualized stromal cells (5×10^4 cells/500 μL per well) were cultured in a 12-well plate in FCS until attaining 50% confluence, and then transfection was performed per the manufacturer's instructions. ILK-siRNA was applied to the cultured cells in conjunction with transfection reagent (vehicle), and fluorescence-conjugated nonspecific siRNA was used as an indicator of transfection efficiency and transfection control. Transfection efficiency was calculated by counting the total number of cells as well as the number of cells transfected by fluorescent-conjugated siRNA at three different low-power fields (×20) under a fluorescent microscope. Unless otherwise stated, cells were treated with siRNA for 24 hours and passaged at 72 hours after transfection. A sample of cells in each group were used for Western blot analysis to determine silencing efficiency.

Western Blot Analysis

Total protein from control and experimentally treated cells was extracted with the use of cell extraction buffer (Pierce) containing 3 mmol/L phenylmethylsulfonyl fluoride and a protease inhibitor cocktail (Sigma). Protein concentration was determined by means of a detergent-compatible protein assay (Bio-Rad Laboratories). Samples (15 μg) were loaded on 10% Tris-HCl Ready Gels (Bio-Rad), electrophoretically separated, and electroblotted onto nitrocellulose membrane (Bio-Rad). The membrane was blocked with 5% nonfat dry milk in TBS containing 0.1% Tween 20 for 1 hour to reduce nonspecific binding. The membrane was then incubated overnight at 4°C with either an ILK mouse monoclonal antibody (Sigma), a total-Akt rabbit polyclonal antibody (Cell Signaling), phospho-Akt (Ser473), a rabbit polyclonal antibody (Cell Signaling), a total-GSK3β (27C10) rabbit monoclonal antibody (Cell Signaling), a phospho-GSK3β (Ser9) (5B3) rabbit monoclonal antibody (Cell Signaling), or a β-actin mouse monoclonal antibody (Santa Cruz Biotechnology) with the use of proper dilutions and gentle agitation. The membranes were then incubated with horseradish peroxidase–conjugated antimouse or antirabbit secondary antibodies (Vector) for 1 hour. Protein was visualized by means of light emission on film (Amersham Biosciences) with the use of enhanced chemiluminescence substrate (Amersham). β-Actin or GAPDH immunostaining was used as an internal control.

Methylthiazolyl Tetrazolium Assay

Numbers of the decidualized ESCs treated with either vehicle, nonspecific transfection control, ILK-siRNA, or protein kinase B (AKT) siRNA for 72 hours in the adhesion function and viability test were measured by means of MTT assay (29), which depends on the reduction of the tetrazolium salt MTT (3-[4,5-dimethylthiazol-2-yl]-2,5-diphenyl tetrazolium bromide; Sigma-Aldrich) by functional mitochondria to formazan. After 4-hour incubation of the cells at 37°C with MTT, acidified isopropanol was added to solubilize the blue crystals, and the intensity was measured colorimetrically at a wavelength of 570 nm, with background subtraction at 650 nm.

Cell Migration and Invasion Assays

A transwell cell migration assay was performed with the use of 24-well chambers with 8-μm pore size polycarbonate filters (Costar). To assess cell invasion, the polycarbonate filters were coated with extracellular matrix (50 μg filter; Sigma Chemical), dried overnight, and rehydrated at room temperature before use for 1 hour (30, 31). In both assays, the cells were trypsinized and resuspended in DMEM/high glucose. ESCs (1×10^5) in 200 μL DMEM/high glucose were seeded on the upper chamber, and DMEM/high glucose of 500 μL containing 10% BMS was placed in the lower chamber. E_2 + P was added to both upper and lower chambers. After incubation for 48 hours at 37°C, the nonmigrating cells in the upper chamber were gently scraped away with a cotton bud, and the cells that migrated through the filters were stained with Giemsa and counted in six representative areas per filter with the use of an Olympus IX71 microscope. The average cell numbers for each specimen were used for analysis.

Immunofluorescent Staining

Experimental cells in each treatment were obtained (4.0×10^4 cells/mL) and seeded onto 8-chamber culture slides (BD Biosciences), cultured for 24 hours, and then fixed with the use of 4% paraformaldehyde for 30 minutes at 4°C. After washing, the slides were incubated with a 1:6,000 dilution of mouse monoclonal anti–human ILK antibody (Sigma) for 60 minutes at room temperature, followed by Texas Red–conjugated donkey anti–mouse IgG (1:150, Jackson Immunoresearch Laboratories) for 30 minutes at room temperature and fluorescein isothiocyanate–conjugated phalloidin (Sigma) for 30 minutes. After treatment with 6-diamino-2-phenylindole (DAPI; Sigma) for 15 minutes and mounted with antifade mounting medium (prepared with 1,4-phenylene-diamine [Sigma], 86% glycerol, and 0.2 mol/L Tris-HCl, pH 8.0), slides were examined with the use of the Axioplan 2 Imaging (Carl Zeiss) system, as detailed above.

Statistical Analyses

Normality was assessed by means of Kolmogorov-Smirnov test. Data in gaussian distribution, including the H-score values, Western blot analyses, and MTT assays, were presented as mean ± SEM and then analyzed with the use of Student *t* test or one-way analysis of variance with post hoc least significant difference (LSD) test for pairwise comparisons between groups. Statistical calculations were performed with the use of SPSS for Windows, release 17.0.0/2008 (IBM-SPSS). Statistical significance was defined as $P<.05$.

RESULTS

Changes of ILK Expressions in Immunohistochemical Staining across the Menstrual Cycle

Significantly higher ILK expression was observed in the round-shaped ESCs of the late-secretory phase endometrium (Fig. 1D) compared with ESCs present in other phases of the cycle, and attained its highest level in the decidual cells of early pregnancy (Fig 1E; $P<.05$ and $P<.01$, respectively; Fig. 1G). Interestingly, ILK expression was located submembranously in some of the decidual cells of early pregnancy (Fig. 1E, arrows). Conversely, endometrial glandular cells

FIGURE 1

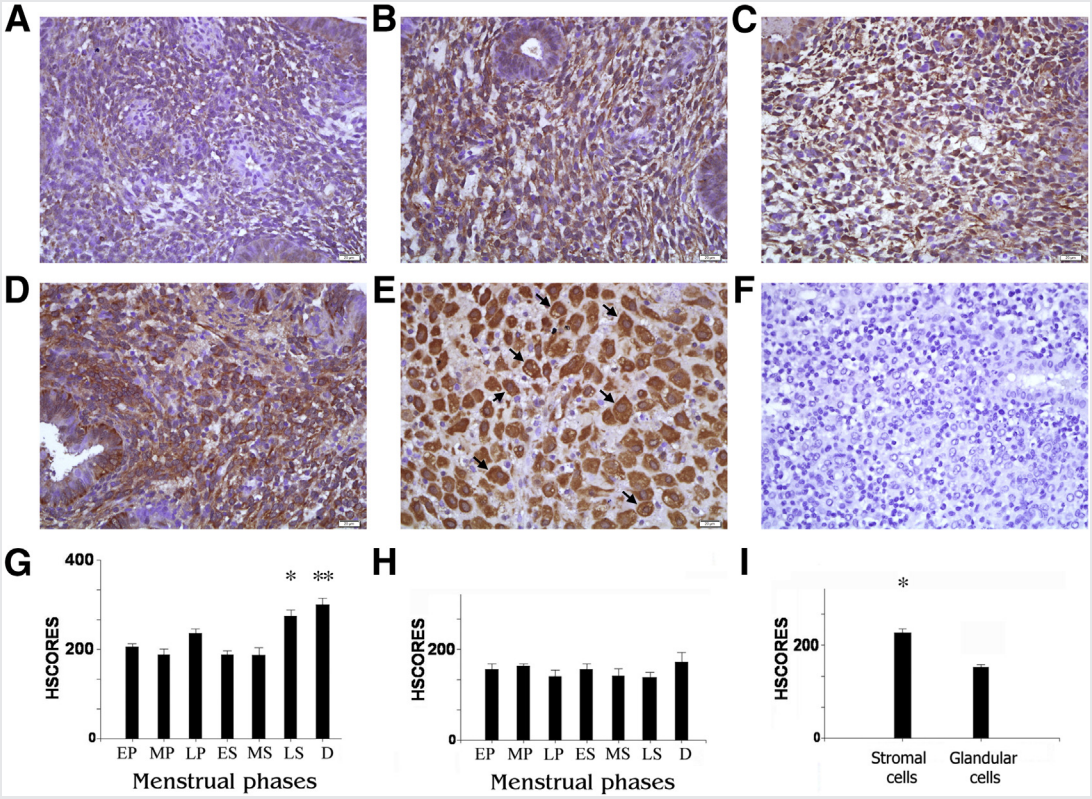

Immunohistochemical staining of integrin-linked kinase (ILK) in endometrium of different menstrual phases and early pregnancy decidua. Representative micrographs are shown with positive signals in brown color. (**A**) Early proliferative (EP) phase; (**B**) late proliferative (LP) phase; (**C**) early secretory (ES) phase; (**D**) late secretory (LS) phase; (**E**) early pregnancy decidua (**D**); (**F**) isotype control (late secretory phase). Note the submembranous-distributed, thicker-stained brownish spots (*arrows*) in some of the polygonal-shaped decidual cells of early pregnancy. ×200; bar = 100 μm. (**G**) H-Scores of ILK in endometrial stromal cells (ESCs; n = 5 for each menstrual phase and early pregnancy; total n = 35; *$P<.05$ vs. all menstrual phases excluding early pregnancy; **$P<.01$ vs. all menstrual phases excluding late secretory phase). (**H**) H-Scores in endometrial glandular cells (EGCs); (**I**) comparison of H-scores of whole menstrual cycle and early pregnancy between ESCs and EGCs (*$P<.05$ vs. EGC). MP = midproliferative; MS = midsecretory.

Yen. ILK and decidualization. Fertil Steril 2016.

(EGCs) displayed significantly lower ILK immunoreactivity than ESCs ($P<.05$; Fig. 1I) and consistently displayed no differences throughout the cycle (Fig. 1H).

ILK Expression in the In Vitro Decidualization of Cultured ESCs

Our initial hypothesis was that ILK expression is regulated by ovarian hormones. To test the existence of nongenomic action of steroid hormones, ESCs were cultured short term with either vehicle, E_2 (10^{-8} mol/L), P (10^{-7} mol/L), or E_2 + P for 15 minutes, 45 minutes, 24 hours, and 48 hours. However, ILK expression did not show any changes among the treatment groups (n = 3; Fig. 2A).

Then, the ESCs underwent in vitro decidualization with E_2 + P for 12 days with prolactin levels in ESC supernates checked on alternate days, as shown in Figure 2B (n = 8). The value obtained on day 6 (1.28 ± 0.30 pg/mL) was significantly higher than on day 0 (0.68 ± 0.04 pg/mL; $P<.05$). The value kept rising and reached a final value of 11.53 ± 3.74 pg/mL on day 12. Notable morphologic changes were seen from day 6, as most of the cells transformed into the typical cobblestone morphology of decidualized ESCs, whereas the cells treated with vehicle remained spindle-shaped and fibroblast-like in appearance (Fig. 2C [day 7]). Consistently, Western blot analysis showed a significant increase in the level of ILK on days 6, 8, and 12 ($P<.05$ compared with day 0; Fig. 2D). However, the ILK yield did not change after day 6, and the level of ILK on day 12 was not different from days 6 and 8 (Fig. 2D).

Morphologic Changes after ILK Knockdown by siRNA Transfection

First-trimester decidual cells (n = 3) were initially treated with vehicle, ILK-siRNA, or nonspecific siRNA used as a transfection control for 72 hours. Decidual cells in the control-transfection group displayed a polygonal appearance with multiple scattered dots of ILK, some of which were observed at the tip of the expanded web-shaped actin fibers (Fig. 3Aa, inset). In contrast, ILK-siRNA–transfected decidual cells displayed a total absence of ILK expression as well as parallel intracellular actin fibers (Fig. 3Ab).

Subsequently, isolated ESCs were subjected to in vitro decidualization and transfection as described above. After 72 hours of incubation, transfection efficiency, measured with the use of fluorescent-labeled siRNA by means of fluorescence microscopy at three different low-power fields (×20), was 73.7% (figure not shown). Identifiable cellular morphologic "reversal" was observed in the ILK-siRNA–treated group, which presented an appearance of predecidualized cells (Fig. 3B). The ILK expression was effectively blocked (Fig. 3Ca), and the knockdown efficiency of ILK-siRNA, as measured with the use of Western blot, was 65.8% compared with transfection control (mean ± SEM: 54.8 ± 10.6 *vs.* 160.4 ± 11.4, respectively; $P<.01$,

FIGURE 2

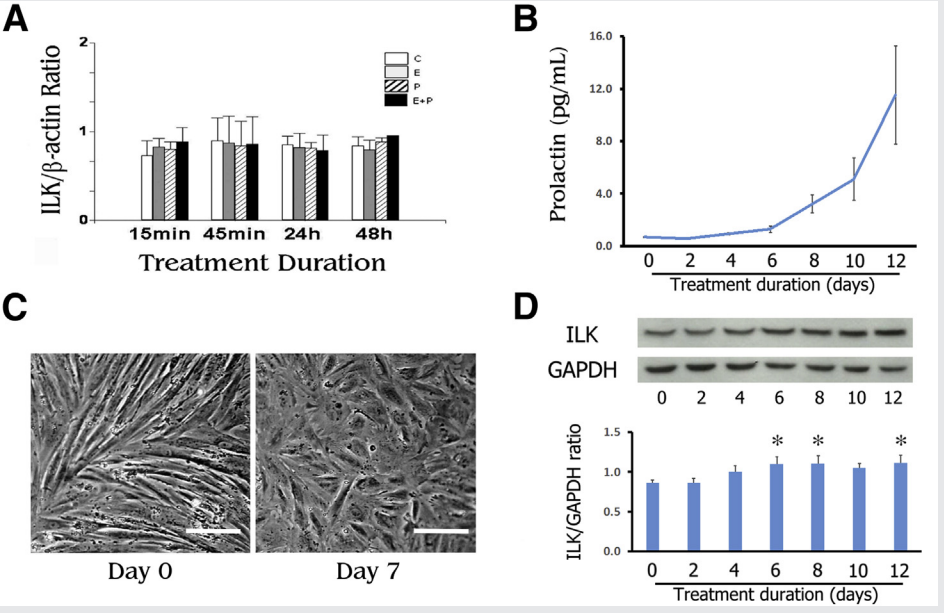

ILK expression in cultured ESCs undergoing in vitro decidualization. (**A**) Densitometry of Western blot analysis. ILK expression in ESCs (n = 3) treated with either vehicle (**C**), E_2 (10^{-8} mol/L), P (10^{-7} mol/L), or E_2 + P for 15 minutes, 45 minutes, 24 hours, and 48 hours. C = control. (**B**) PRL values along with the course of in vitro decidualization (E_2 + P treatment for 12 days) in the supernate of ESC cultures (n = 8). (**C**) Morphologic changes of the cultured ESCs undergoing in vitro decidualization. On day 0, cells showed a typical spindle-shaped fibroblast-like morphology; however, on day 7, the majority of the cells were transformed into a typical polygonal cobblestone-like morphology of decidualization. ×200; bar = 100 μm. (**D**) Western blot analysis of ILK expression in the lysates of ESCs undergoing in vitro decidualization for 12 days (n = 8; *$P<.05$ vs. day 0). All results are presented as mean ± SEM. Abbreviations as in Figure 1.

Yen. ILK and decidualization. Fertil Steril 2016.

FIGURE 3

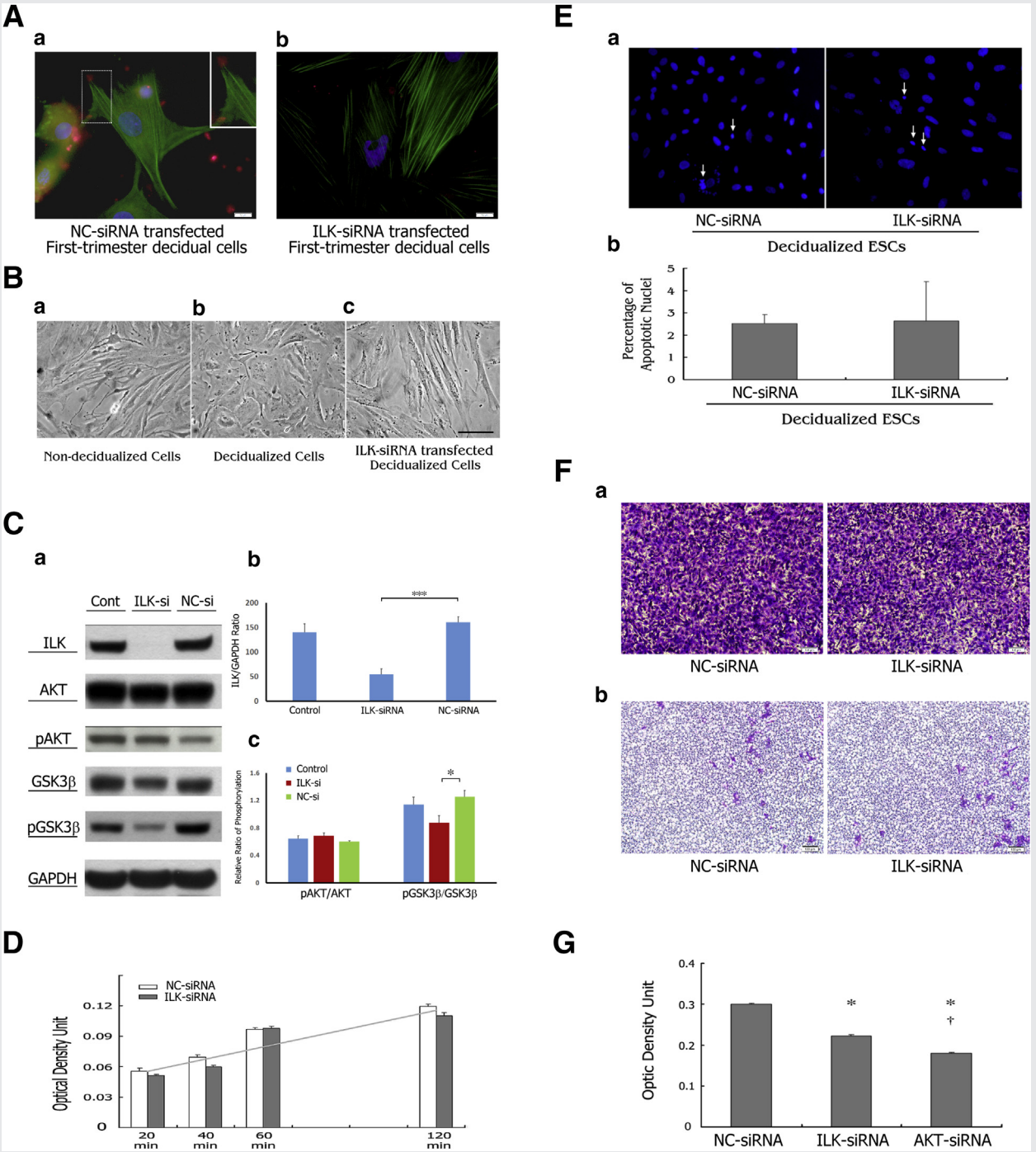

Effects of ILK knockdown with small interfering (si) RNA transfection. (**A**) The first-trimester decidual cells were treated with either vehicle, ILK-siRNA, or a control transfection of nonspecific siRNA for 72 hours. The immunofluorescent staining demonstrates the decidual cells transfected with (**a**) nonspecific control (NC) and (**b**) ILK-siRNA in relation to the ILK protein (Texas Red labeled, *red*) and the actin stress fibers (fluorescein isothiocyanate [FITC] labeled, *green*). Cell nuclei were stained with 6-diamino-2-phenylindole (DAPI, *blue*). Inset in (**a**) shows the linkage of ILK protein with the wide expanded actin fibers (n = 3; ×1,000; bar = 10 μm). (**B–G**) Then the isolated ESCs underwent in vitro decidualization for 8 days and were incubated with either vehicle, ILK-siRNA, or nonspecific siRNA for 72 hours. (**B**) Morphology of (**a**) ESCs before decidualization, (**b**) decidualized ESCs undergoing nonspecific siRNA transfection, and (**c**) decidualized ESCs undergoing ILK-siRNA transfection (×200; bar = 100 μm). (**C**) (**a**) The cell lysates of the above-mentioned ESCs were tested with the use of Western blot analysis of ILK expression and the phosphorylation of protein kinase B (AKT) and glycogen synthase kinase (GSK) 3β; (**b**) bar chart of ILK/GAPDH ratios; (**c**) relative ratios of phosphorylated/total AKT and GSK3β (n = 5; * P<.05, ***P<.001 vs. control). (**D**) The transfected decidualized ESCs were passaged and cultured for 20 minutes, 40 minutes, 60 minutes, and 120 minutes. The relative quantities of adhesion cells were assessed by means of methylthiazolyl tetrazolium (MTT) assay (n = 8; no significant differences [NS]). (**E**) Apoptosis of the

Fig. 3Cb). No difference was observed between cells treated with transfection control or with vehicle (140.2 ± 17.5).

Functional Analyses of the siRNA-Treated Decidualized ESCs

Because ILK is a potential upstream kinase in either Akt or GSK3β signaling pathways, Western blot analysis was used to determine potential signaling elicited by ILK in decidualized ESCs (Fig. 3C). Significantly decreased phosphorylation ratio of GSK3β was noted in ILK-knockdown cells compared with transfection control cells (0.88 ± 0.10 vs. 1.25 ± 0.09, respectively; $P<.05$; Fig. 3Cc). However, no difference in the phosphorylation ratio of Akt was observed after ILK knockdown (0.69 ± 0.04 vs. 0.60 ± 0.01, respectively). Furthermore, control transfection did not compromise phosphorylation ratios compared with vehicle control (Fig. 3Cc).

Numbers of adhesion cells were measured by culturing the cells in a 96-well plate (2×10^4 cells/well) for 20, 40, 60, and 120 minutes and use of MTT assay after washing out the nonadherent cells. The average quantity of adherent cells showed no differences between the control and ILK-siRNA–transfected decidualized ESCs ($P=.451$). However, a linear increase was observed throughout 2 hours of incubation in both groups (Fig. 3D).

Karyopyknosis and nuclear fragmentation, which are early morphologic indicators of apoptosis, were measured by means of DAPI staining of the transfected decidualized ESCs and counted with the use of fluorescence microscopy (27) (Fig. 3Ea). Few apoptotic cells were noted, with similarly low apoptotic rates (0.025 ± 0.004 vs. 0.026 ± 0.018, respectively; $P=.953$; Fig. 3Eb), in both groups from the analysis of five different low-power fields (×20) in each slide.

In the transwell migration assay, abundant decidualized ESCs transfected with either ILK-siRNA or control migrated through the micropores of the uncoated filters. The cell numbers/area were similar in both groups (83.8 ± 2.9 vs. 93.2 ± 5.3, respectively; $P=.258$; Fig. 3Fa), although ILK-siRNA–transfected ESCs appeared to be slimmer than ESCs transfected with nonspecific control. However, use of filters coated with extracellular matrix revealed that, for both groups, similar small numbers of decidualized ESCs were observed to invade through the filters (Fig. 3Fb).

Viability of decidualized ESCs was measured by MTT assay after control transfection or transfection with ILK-siRNA or Akt-siRNA, followed by 72 hours of culture (Fig. 3G). The MTT results revealed a significant decrease in cell survival of the ILK-siRNA–treated group compared with the transfection control group (0.223 ± 0.003 vs. 0.300 ± 0.003; $P<.05$). Akt-siRNA transfection further decreased cell survival to an even lower level (0.180 ± 0.002), which was significantly different from either decidualized ESCs undergoing ILK knockdown ($P<.05$) or transfection control ($P<.05$; Fig. 3G).

Interactions of ILK with Actin Stress Fibers

Immunofluorescence staining demonstrated colocalization of ILK with intracellular actin stress fibers on cultured ESCs (Fig. 4). Specifically, ILK staining in decidualized ESCs (Fig. 4B) displayed notably higher expression, which was detected in focal submembranous points at the ends of F-actin stress fibers versus nondecidualized ESCs (Fig. 4A). In nondecidualized ESCs, intracellular ILK was observed in trace amounts, with scant amounts of actin fibers that appeared to be thinner and in parallel arrangement, which gave the cells a leaner, fibroblast-like shape. Conversely, actin stress bundles in decidualized ESCs (Fig. 4B) were notably thicker, more abundant, and arranged in an expanded organized fashion, which gave the decidualized cells a typical polygonal shape.

This contrast in morphology was also observed in the ILK-siRNA–treated cells. In ~80% of cells that were successfully treated with ILK-siRNA, ILK expression was significantly decreased, with numbers of frail-appearing actin fibers observed in a "lazy" and loose-shape arrangement, and the cells reverted into an undecidualized appearance (Fig. 4C, arrows). In contrast, the few cells that failed to be transfected maintained elevated expression of subcortical ILK as well as their expanded-shape actin stress bundles, which were highly organized, and preserved their polygonal appearance (Fig. 4C, arrowhead).

DISCUSSION

To our knowledge, this is the first study that describes the temporal and spatial relationship of ILK expression during endometrial decidualization. The resulting new in vivo observations reveal up-regulation of submembranous-distributed ILK in stromal cells during specific times of decidual transformation (Fig. 1). Strong evidence is also offered that increased expression of ILK is essential for the reorganization of the actin cytoskeleton that drives the morphologic transformation of ESCs from a fibroblast-like appearance to the cobblestone-like decidual cell phenotype (Fig. 4) and positively regulates cell survival (Fig. 3G).

Ovarian hormones regulated expression of ILK in ESCs during in vitro decidualization, which revealed increased expression of ILK in conjunction with decidualization-related

FIGURE 3 Continued

transfected decidualized ESCs were assessed with the use of DAPI staining. (**a**) Arrows indicate apoptotic signs of pyknotic or fragmented nuclei. (**b**) Relative ratios of apoptotic nuclei (n = 5; NS). (**F**) Representative micrographs show the transfected decidualized ESCs with Giemsa stain on the filters of transwell assay in (**a**) migration and (**b**) invasion tests (n = 3; ×100; bar = 100 μm). (**G**) The relative quantities of survived cells by MTT assay were measured on the decidualized ESCs treated with nonspecific transfection control, ILK-siRNA, or AKT-siRNA and cultured for 72 hours (n = 8; *$P<.05$ vs. control; †$P<.05$ vs. ILK-siRNA). All results are presented as mean ± SEM. Cont = vehicle control, decidualized ESCs incubated with transfection reagent; other abbreviations as in Figure 1.

Yen. ILK and decidualization. Fertil Steril 2016.

FIGURE 4

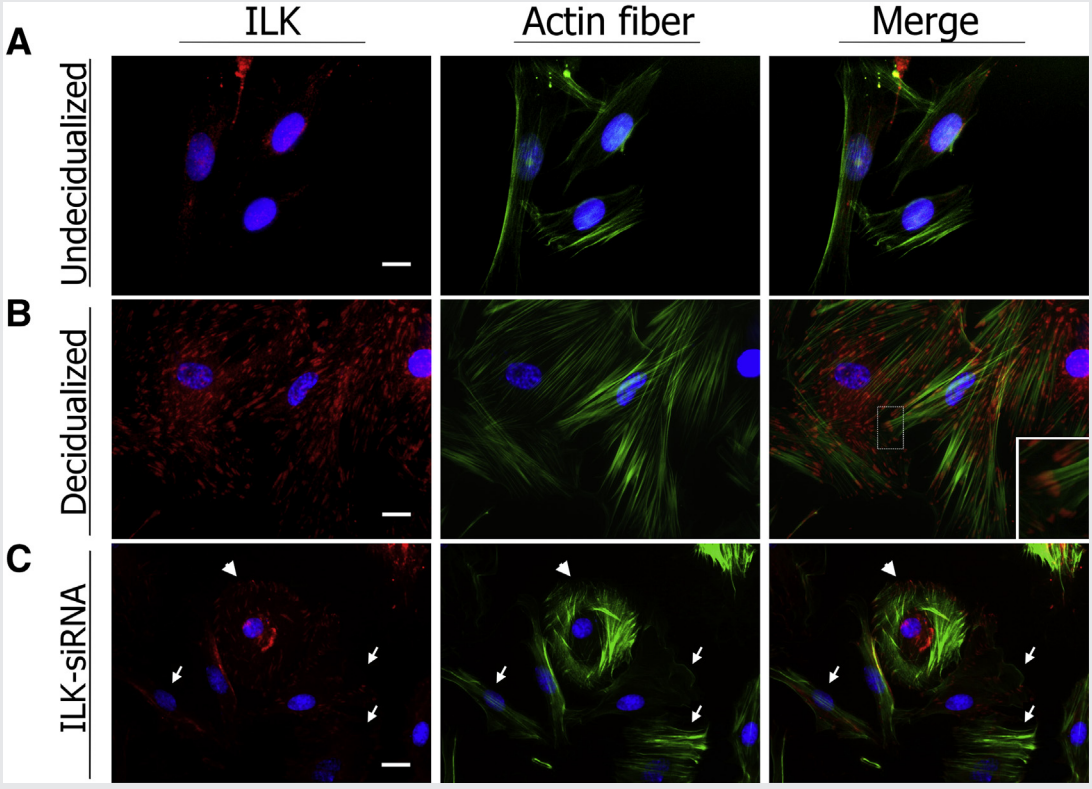

Colocalization of ILK distribution and actin fiber. Immunofluorescent staining shows the ILK protein (Texas Red labeled, *red*), and the actin stress fibers (FITC labeled, *green*) in the (**A**) undecidualized ESCs, (**B**) decidualized ESCs, and (**C**) ILK-siRNA–treated decidualized ESCs. Cell nuclei were stained with 6-diamino-2-phenylindole (DAPI) and are shown in *blue*. Inset in (**B**) shows a magnified picture from the boxed area, in which the marked increased ILK protein in the cortical area is linked to the tips of the wide expended actin fibers. (**C**) Decidualized cells in which ILK was successfully knocked down (*arrow*) showed faint and scanty spots of ILK and an elongated cell morphology with parallell-arranged array of actin fibers. Cells that failed to be transfected by ILK-siRNA (*arrowhead*) preserved their polygonal-shaped organization of actin fibers with many spots of ILK protein located at their tips. ×1,000; bar = 10 μm. Abbreviations as in Figures 1 and 3.

Yen. ILK and decidualization. Fertil Steril 2016.

morphologic changes (Fig. 2C). This ovarian steroid hormone–induced expression is likely regulated through a "classic" genomic steroid hormone action, because a minimum of 6 days is required to induce a significant increase in ILK production. Expression of ILK expression was predominantly localized in the stromal cells, and virtually absent in glandular epithelial cells, suggesting an endometrial stromal cell–specific role of ILK. During the late secretory phase of the menstrual cycle, ESCs become prominent whereas glandular epithelial cells shrink (Fig. 1).

In addition to its well described role in connecting integrin to the actin cytoskeleton, ILK can also transmit signals through the Akt and/or GSK3β pathways (32). Previous studies found that ILK could phosphorylates and activates Akt at Ser 473, which regulates specific genes essential for cell survival (33, 34), and that ILK could directly phosphorylate GSK3β at Ser 9, thereby leading to activation of such transcription factors as β-catenin/T cell transcription factor (Tcf), and cyclic adenosine monophosphate (cAMP) response element-binding protein (CREB), which stimulate cell proliferation (7, 33). However, knockdown of ILK in the present study significantly decreased GSK3β, but not Akt, phosphorylation (Fig. 3B), suggesting that ILK in decidualized ESCs transmit signals through the GSK3β, but not the Akt, pathway. Because a recent study also found that reduced GSK3β expression led to the reduction of proliferation of uterine myometrial cells (35), the significantly decreased numbers of the decidualized ESCs with effective ILK knockdown in the present study (Fig. 3G) suggest that ILK may play a role in cellular proliferation by acting through the GSK3β signaling pathway. Because the Akt pathway usually plays an essential role in cell survival, treatment with Akt-siRNA further decreased numbers of decidualized ESCs, which differed significantly from the result of treatment with ILK-siRNA (Fig. 3G). This finding supported the speculation that Akt signaling may not play an active role in the ILK functions in decidualized ESCs (Fig. 3B).

The present study did not detect any positive correlation between ILK signaling with either cell adhesion (Fig. 3D), apoptosis (Fig. 3E), migration (Fig. 3Fa), or invasion (Fig. 3Fb) functions in decidualized ESCs. The explanation of why ILK is not the key regulator of these functions in decidual cells may reside in key differences in physiologic

characteristics of decidual cells compared with those of aggressively invasive cells. Although ILK has been suggested as a molecular marker of epithelial-to-mesenchymal transition, that suggestion was generally derived from studies of cancer cells (30, 36) or in situations of pathologic overexpression of ILK (7, 8, 37). Because the decidua acts as a barrier at the maternal site of the placenta-fetal interface, we don't think that the increased decidual ILK expression could suggest a physiologic function of increased migration or invasion of decidual cells, as has been noted in studies of chorionic villi (15), endometriosis (17), and cancer cells (3, 33).

The role played by ILK in regulating actin polymerization (4) and organization was clearly demonstrated in the present study (Fig. 4). The submembranous localization of ILK is consistent with a physiologic role in governing G-actin polymerization, and/or F-actin bundle formation (38), which contribute to the polygonal appearance of decidual cells. Consistently with previous studies (39, 40), ILK knockdown caused depolymerization of actin filaments, indicated by markedly decreased numbers of actin fibers in the majority of decidual cells (Fig 3Ab and Fig. 4C). Furthermore, knockdown of ILK abolished morphologic transformation of decidual cells (Fig. 4C), thus providing strong evidence for the role of ILK in decidualization of ESCs.

A potential limitation of this study may lie in the dating of endometrial specimens (Fig. 1) by last menstrual period and morphology at the time of collection, because more precise methods of dating of tissues are currently used. A more important limitation is inherent in missing pieces of the puzzle between the correlation of circulating levels of steroid hormones with the production of ILK. Specifically, there is no clear explanation as to why ILK expression increases at the 6th day of in vitro decidualization of ESCs when in situ observations indicate significantly elevated ILK expression in the late secretory phase, which corresponds to a decline in circulating progesterone levels, as well as in the decidua of early pregnancy, which corresponds to elevated circulating progesterone levels. A potential explanation for this apparent disparity is that progesterone does not directly affect ILK production and that some as yet unrevealed factor plays a more important role during decidualization. Because the evaluation of integrin expression was beyond the scope of the present study, we are also not sure if the constitutively increased ILK expression could be a result of integrin switching, given that integrin $\beta 1$ presents in stromal cells since the midsecretory phase, increases at the time of implantation, and sustains the level to early pregnancy (18, 41). Nevertheless, the increase of ILK is essential for the morphologic transformation of endometrial stromal cells during decidualization, with further corroboration required to determine a definite role for this increase in ILK expression as well as the mechanism by which the ILK works during decidualization.

In conclusion, significantly increased ILK expression in the mid-late secretory phase enables ILK to play a pivotal role in driving the morphologic transformation of ESCs into the typical polygonal appearance through the organization of the actin cytoskeleton during decidualization. Blockage of ILK expression resulted in the morphologic reversal of decidual cells. Transmission of signals through the GSK3β pathway may enable ILK to contribute to cell proliferation during decidualization. Complementing the documented role of ILK in human malignancies, the present study provides the first demonstration that ILK is an important mediator of endometrial cell functions in preparation for reproduction. Further studies are necessary to explore the potential mechanism of ILK signaling during decidualization and implantation.

Acknowledgments: The authors thank Hakan Cakmak, M.D., for his technical consultation, William Murk, MSc, Ph.D., and Abhishek Mangeshikar, M.D., for their editorial assistance in writing the manuscript, Tzu-Ti Shaw, M.S., and Pei-Chia Yang, M.S., for their great contributions in technical assistance, and Frederick Schatz, Ph.D., for his assistance with critical reading and the language editing of the manuscript.

REFERENCES

1. Kayisli UA, Korgun ET, Akkoyunlu G, Arici A, Demir R. Expression of integrin alpha5 and integrin beta4 and their extracellular ligands fibronectin and laminin in human decidua during early pregnancy and its sex steroid-mediated regulation. Acta Histochem 2005;107:173–85.
2. Hynes RO. Integrins: versatility, modulation, and signaling in cell adhesion. Cell 1992;69:11–25.
3. Hannigan G, Troussard AA, Dedhar S. Integrin-linked kinase: a cancer therapeutic target unique among its ILK. Nat Rev Cancer 2005;5:51–63.
4. Brakebusch C, Fassler R. The integrin-actin connection, an eternal love affair. EMBO J 2003;22:2324–33.
5. Grashoff C, Thievessen I, Lorenz K, Ussar S, Fassler R. Integrin-linked kinase: integrin's mysterious partner. Curr Opin Cell Biol 2004;16:565–71.
6. Yen CF, Wang HS, Lee CL, Liao SK. Roles of integrin-linked kinase in cell signaling and its perspectives as a therapeutic target. J Minim Invasive Gynecol 2014;3:67–72.
7. Oloumi A, McPhee T, Dedhar S. Regulation of E-cadherin expression and beta-catenin/Tcf transcriptional activity by the integrin-linked kinase. Biochim Biophys Acta 2004;1691:1–15.
8. Gil D, Ciolczyk-Wierzbicka D, Dulinska-Litewka J, Zwawa K, McCubrey JA, Laidler P. The mechanism of contribution of integrin linked kinase (ILK) to epithelial-mesenchymal transition (EMT). Adv Enzyme Regul 2011;51:195–207.
9. Huang BS, Tsai HW, Wang PH, Twu NF, Yen MS, Chen YJ. Epithelial-to-mesenchymal transition in the development of adenomyosis. J Minim Invasive Gynecol 2015;4:55–60.
10. Hay ED. The mesenchymal cell, its role in the embryo, and the remarkable signaling mechanisms that create it. Dev Dyn 2005;233:706–20.
11. Thiery JP, Sleeman JP. Complex networks orchestrate epithelial-mesenchymal transitions. Nat Rev Mol Cell Biol 2006;7:131–42.
12. Sakai T, Li S, Docheva D, Grashoff C, Sakai K, Kostka G, et al. Integrin-linked kinase (ILK) is required for polarizing the epiblast, cell adhesion, and controlling actin accumulation. Genes Dev 2003;17:926–40.
13. Lynch DK, Ellis CA, Edwards PA, Hiles ID. Integrin-linked kinase regulates phosphorylation of serine 473 of protein kinase B by an indirect mechanism. Oncogene 1999;18:8024–32.
14. Troussard AA, Tan C, Yoganathan TN, Dedhar S. Cell–extracellular matrix interactions stimulate the AP-1 transcription factor in an integrin-linked kinase- and glycogen synthase kinase 3-dependent manner. Mol Cell Biol 1999;19:7420–7.
15. Elustondo PA, Hannigan GE, Caniggia I, MacPhee DJ. Integrin-linked kinase (ILK) is highly expressed in first trimester human chorionic villi and regulates migration of a human cytotrophoblast–derived cell line. Biol Reprod 2006;74:959–68.

16. Cui K, Yan T, Luo Q, Zheng Y, Liu X, Huang X, et al. Ultrasound microbubble–mediated delivery of integrin-linked kinase gene improves endothelial progenitor cells dysfunction in pre-eclampsia. DNA Cell Biol 2014;33:301–10.
17. Zheng Q, Xu Y, Lu J, Zhao J, Wei X, Liu P. Emodin inhibits migration and invasion of human endometrial stromal cells by facilitating the mesenchymal-epithelial transition through targeting ILK. Reprod Sci 2016;23:1526–35.
18. Sueoka K, Shiokawa S, Miyazaki T, Kuji N, Tanaka M, Yoshimura Y. Integrins and reproductive physiology: expression and modulation in fertilization, embryogenesis, and implantation. Fertil Steril 1997;67:799–811.
19. Lessey BA, Damjanovich L, Coutifaris C, Castelbaum A, Albelda SM, Buck CA. Integrin adhesion molecules in the human endometrium. Correlation with the normal and abnormal menstrual cycle. J Clin Invest 1992;90:188–95.
20. Lessey BA, Castelbaum AJ, Buck CA, Lei Y, Yowell CW, Sun J. Further characterization of endometrial integrins during the menstrual cycle and in pregnancy. Fertil Steril 1994;62:497–506.
21. Han CM, Wu KY, Su H, Huang CY, Wu PJ, Wang CJ, et al. Feasibility of transumbilical single-port laparoscopic hysterectomy using conventional instruments. J Minim Invasive Gynecol 2014;3:47–9.
22. Wu CJ, Tseng CW, Wu MP. Laparoscopic subtotal hysterectomy in the era of minimally invasive surgery. J Minim Invasive Gynecol 2015;4:8–13.
23. Noyes RW, Hertig AT, Rock J. Dating the endometrial biopsy. Am J Obstet Gynecol 1975;122:262–3.
24. Aghajanova L, Hamilton A, Kwintkiewicz J, Vo KC, Giudice LC. Steroidogenic enzyme and key decidualization marker dysregulation in endometrial stromal cells from women with versus without endometriosis. Biol Reprod 2009;80:105–14.
25. Budwit-Novotny DA, McCarty KS, Cox EB, Soper JT, Mutch DG, Creasman WT, et al. Immunohistochemical analyses of estrogen receptor in endometrial adenocarcinoma using a monoclonal antibody. Cancer Res 1986;46:5419–25.
26. Arici A, Head JR, MacDonald PC, Casey ML. Regulation of interleukin-8 gene expression in human endometrial cells in culture. Mol Cell Endocrinol 1993;94:195–204.
27. Kayisli UA, Selam B, Guzeloglu-Kayisli O, Demir R, Arici A. Human chorionic gonadotropin contributes to maternal immunotolerance and endometrial apoptosis by regulating Fas-Fas ligand system. J Immunol 2003;171:2305–13.
28. Losel R, Wehling M. Nongenomic actions of steroid hormones. Nat Rev Mol Cell Biol 2003;4:46–56.
29. Mosmann T. Rapid colorimetric assay for cellular growth and survival: application to proliferation and cytotoxicity assays. J Immunol Methods 1983;65:55–63.
30. Xing Y, Qi J, Deng S, Wang C, Zhang L, Chen J. Small interfering RNA targeting ILK inhibits metastasis in human tongue cancer cells through repression of epithelial-to-mesenchymal transition. Exp Cell Res 2013;319:2058–72.
31. Chen YJ, Li HY, Chang YL, Yuan CC, Tai LK, Lu KH, et al. Suppression of migratory/invasive ability and induction of apoptosis in adenomyosis-derived mesenchymal stem cells by cyclooxygenase-2 inhibitors. Fertil Steril 2010;94:1972–9.e1–4.
32. Hannigan GE, McDonald PC, Walsh MP, Dedhar S. Integrin-linked kinase: not so "pseudo" after all. Oncogene 2011;30:4375–85.
33. McDonald PC, Fielding AB, Dedhar S. Integrin-linked kinase—essential roles in physiology and cancer biology. J Cell Sci 2008;19:3121–32.
34. Persad S, Attwell S, Gray V, Delcommenne M, Troussard A, Sanghera J, et al. Inhibition of integrin-linked kinase (ILK) suppresses activation of protein kinase B/Akt and induces cell cycle arrest and apoptosis of PTEN-mutant prostate cancer cells. Proc Natl Acad Sci U S A 2000;97:3207–12.
35. Janjusevic M, Greco S, Islam MS, Castellucci C, Ciavattini A, Toti P, et al. Locostatin, a disrupter of Raf kinase inhibitor protein, inhibits extracellular matrix production, proliferation, and migration in human uterine leiomyoma and myometrial cells. Fertil Steril 2016;106:1530–8.e1.
36. Tiwari N, Gheldof A, Tatari M, Christofori G. EMT as the ultimate survival mechanism of cancer cells. Semin Cancer Biol 2012;22:194–207.
37. Medici D, Nawshad A. Type I collagen promotes epithelial-mesenchymal transition through ILK-dependent activation of NF-kappaB and LEF-1. Matrix Biol 2010;29:161–5.
38. Matsudaira P. Actin crosslinking proteins at the leading edge. Semin Cell Biol 1994;5:165–74.
39. Yamaji S, Suzuki A, Kanamori H, Mishima W, Yoshimi R, Takasaki H, et al. Affixin interacts with alpha-actinin and mediates integrin signaling for reorganization of F-actin induced by initial cell-substrate interaction. J Cell Biol 2004;165:539–51.
40. Graness A, Giehl K, Goppelt-Struebe M. Differential involvement of the integrin-linked kinase (ILK) in RhoA-dependent rearrangement of F-actin fibers and induction of connective tissue growth factor (CTGF). Cell Signal 2006;18:433–40.
41. Lessey BA, Castelbaum AJ. Integrins and implantation in the human. Rev Endocr Metab Disord 2002;3:107–17.